Surface Science 602 (2008) 3000–3005

Contents lists available at ScienceDirect

Surface Science

journal homepage: www.elsevier.com/locate/susc

Dissociative adsorption and thermal evolution of carbon tetrachloride on Si(1 1 1)7 × 7

V. Venugopal, M. Ebrahimi, Z.H. He, K.T. Leung *

WATLab, Department of Chemistry, University of Waterloo, Waterloo, Ontario, Canada N2L 3G1

ARTICLE INFO

Article history:
Received 20 June 2008
Accepted for publication 28 July 2008
Available online 12 August 2008

Keywords:
Electron energy loss spectroscopy
Vibrational and electronic spectra
Thermal evolution
Si(1 1 1)7 × 7
Carbon tetrachloride

ABSTRACT

The adsorption of CCl_4 on Si(1 1 1)7 × 7 at room temperature has been characterized by electronic and vibrational electron energy loss spectroscopy (EELS). CCl_4 was found to adsorb dissociatively on Si(1 1 1)7 × 7 with the formation of Si—Cl bond and adsorbed CCl_x species. At high exposures, CCl_4 appears to more readily undergo a greater degree of dechlorination. Using a $Si_{16}H_{18}$ cluster to model only the adatom–restatom site, our density functional theory calculations suggest two plausible adstructures involving the dissociated Cl and CCl_3 fragments. The wavenumbers of the observed EELS features are found to be in general accord with the corresponding calculated wavenumbers. Thermal evolution of the adsorbed fragments has been followed by both vibrational and electronic EELS as a function of the sample annealing temperature. A new EELS feature at 920–960 cm^{-1} attributed to SiC film or alloy formation is found to emerge at 573 K, while the Si—Cl stretch at 550 cm^{-1}, corresponding to dissociated surface Cl, is removed upon annealing to ~883 K. Furthermore, the electronic EELS spectra reveal an energy loss at 9.3 eV that can be assigned to a single-electron transition from the Cl(p_z) bonding state to the Cl(p_z) antibonding state produced by the Si—Cl bond.

1. Introduction

Carbon tetrachloride (CCl_4) is an important process-chemical used in many industrial applications, including chemical vapour deposition of diamond [1], and reactive ion etching for microelectronics devices [2,3]. The interactions of CCl_4 with a semiconductor surface have attracted a lot of attention because CCl_4 is not only a useful surface etching reagent but also an effective carbon doping source for semiconductors. In particular, the adsorption, etching and photo-induced reactions of CCl_4 on Si(1 0 0) have been studied by French et al. [4], who reported that CCl_4 undergoes initial dissociative adsorption at 175 K, followed by multilayer formation at higher exposures. Later, Junker et al. studied the thermal and electron activated reactions of CCl_4 on clean and H-terminated Si(1 0 0) [5], and on oxidized Si(1 0 0) [6]. They found that CCl_4 adsorbs dissociatively on clean Si(1 0 0) even at 100 K, with the formation of Si—Cl surface bonds. Using secondary ion mass spectrometry, Wee et al. [7] studied the effect of simultaneous Ar^+ ion sputtering on the reaction rate of CCl_4 on Si(1 0 0) at room temperature (RT). Moreover, on GaAs (1 1 0) surfaces, Liberman et al. [8] reported molecular adsorption of CCl_4 below 160 K and that dissociation could only be initiated by ultraviolet laser and visible light illumination.

As first elucidated by Takayanagi et al. [9], the Si(1 1 1)7 × 7 surface offers an interesting reconstructed surface structure with 19 dangling bonds distributed over 12 adatoms, 6 rest atoms, and 1 corner atom of the 7 × 7 unit cell. Although the Si(1 1 1)7 × 7 surface generally appears to be more complex than the Si(1 0 0)2 × 1 surface, the 7 × 7 surface offers an important complementary testing ground of directional bonding over a number of spatially and electronically inequivalent reactive sites. There has been a limited number of studies on the interactions of Si(1 1 1)7 × 7 with small chlorinated molecules, including HCl [10] using electronic electron energy loss spectroscopy (EELS), and perchloroethylene and trichloroethylene [11], 1,1-dichloroethylene and monochloroethylene [12], and *iso*-, *cis*- and *trans*-dichloroethylene [13] by using vibrational EELS. In particular, HCl was found to adsorb molecularly at RT and to subsequently dissociate by Miyamura et al. [10]. Our earlier studies on the interactions of chloroethylenes with Si(1 1 1)7 × 7 reveal a few common features, including dechlorination upon RT adsorption with the formation of Si—Cl bond, the formation of hydrocarbon fragments and/or SiC upon further annealing of the adsorbed species, and the desorption of etching product $SiCl_2$ over 800–950 K [11–13]. To our knowledge, the surface chemistry of CCl_4 on Si(1 1 1)7 × 7 has not been reported. It would be especially interesting to compare the reactivity of CCl_4 with those of not only other chlorinated hydrocarbons but also other tetrahedrally coordinated systems on Si substrates. For instance, while CH_4 [14], CF_4 [15], and CH_3Cl [16] appear to be relatively non-reactive towards Si(1 1 1)7 × 7 at RT, $SiCl_4$ [17] undergoes total dissociative chemisorption on Si(1 1 1)7 × 7 at RT with only SiCl found on the surface. In the present work, we study

* Corresponding author.
E-mail address: tong@uwaterloo.ca (K.T. Leung).

0039-6028/$ - see front matter © 2008 Elsevier B.V. All rights reserved.
doi:10.1016/j.susc.2008.07.038

the RT adsorption of CCl_4 on Si(1 1 1)7 × 7 as a function of exposure and follow the thermal evolution by using both vibrational and electronic EELS. The density functional theory (DFT) calculations have been performed to determine the plausible adsorption structures, and their corresponding vibrational wavenumbers are compared with the EELS data.

2. Experimental details

The experimental apparatus and the procedure used in the present work have been described in detail elsewhere [18]. Briefly, the experiments were conducted in a home-built ultrahigh vacuum system with a base pressure of 1×10^{-10} Torr. Unless mentioned otherwise, all of the EELS measurements were conducted using a custom-built EELS spectrometer described previously [18] with the sample held at RT under specular reflection scattering at 45° from the surface normal. A routine energy resolution of 15 meV (or 120 cm^{-1}) full width at half maximum (FWHM) with a typical count rate of 50,000 counts/s for the elastic peak could be achieved with our spectrometer operating at 5 eV impact energy. It should be noted that the calibration and tuning of the EELS spectrometer typically limit the reproducibility of the measured peak positions to ~2 meV (or 16 cm^{-1}) in the present work. For electronic EELS measurements, an impact energy of 100 eV was used, with a resolution of 40 meV FWHM and a typical count rate of 90,000 counts/s for the elastic peak.

The Si(1 1 1) sample (p-type boron-doped, 40 Ω cm, 8 × 6 mm^2, 0.5 mm thick) with a stated purity of 99.999% was purchased from Virginia Semiconductor Inc. The sample was mechanically fastened to a Ta sample plate with 0.25-mm-diameter Ta wires and could be annealed by electron bombardment from a heated tungsten filament at the backside of the sample. The Si(1 1 1) sample was cleaned by a standard procedure involving repeated cycles of Ar^+ sputtering (1.5 kV, 4.2 μA/cm^2 for 30 min) and annealing to 1200 K until a sharp 7 × 7 low-energy electron diffraction pattern was observed. The cleanliness of the 7 × 7 surface was further verified in situ by the lack of any detectable vibrational EELS feature attributable to surface contamination from the ambient, particularly the Si—C stretching mode at 800–850 cm^{-1}. Carbon tetrachloride (Aldrich, 99.7% purity) was used without further purification after appropriate degassing by repeated freeze–pump–thaw cycles. The clean Si(1 1 1) sample was exposed to the CCl_4 vapour at a typical pressure of 1–4 × 10^{-7} Torr by using a variable leak valve.

3. Results and discussion

3.1. Room temperature adsorption of CCl_4 on Si(1 1 1)7 × 7

Fig. 1 shows the EELS spectra of the Si(1 1 1)7 × 7 surface exposed to different doses of CCl_4 at RT. We also compare the present observed vibrational modes of CCl_4 adsorbed on Si(1 1 1)7 × 7 with that on Ni(1 1 0) [19] and with gas-phase isolated molecule data [20] in Table 1. Evidently, two broad features below 1000 cm^{-1} are observed. In particular, the broad feature at 550 cm^{-1} (Fig. 1a) can be attributed to the Si—Cl stretching mode, in good accord with the positions of those observed for chlorinated hydrocarbons on Si(1 1 1)7 × 7 (510 cm^{-1}) [11–13], Cl_2 on Si(1 0 0)2×1 (553–600 cm^{-1}) [21], and Cl-terminated Si(1 1 1) (580 cm^{-1}) [22]. The intensity of the overtone of this Si—Cl stretching mode (expected at ~1020 cm^{-1}) is found to be too weak to be observed [21]. The instrument resolution does not allow us to identify the specific existence of di-, tri-, or tetrachloride, if any, on the surface, which are expected to produce symmetric and asymmetric Si—Cl stretching mode at 376–458 cm^{-1} and 533–616 cm^{-1}, respectively, and a deformation mode at 145–229 cm^{-1} [21]. In addition, the broad peak near 820 cm^{-1} is attributed to contributions from the C—Cl and Si—C stretching modes. This assignment is consistent with the location of the C—Cl stretching mode found for the gas-phase CCl_4 (776 cm^{-1}) [20] and infrared bands for the CCl_x adspecies (750–800 cm^{-1}) on CaO [23]. In the EELS study of CCl_4 on Ni(1 1 0), Chesters and Lennon [19] have assigned the feature at 720 cm^{-1} to C—Cl stretching mode resulting from partial dissociation of CCl_4. We also obtain by DFT calculations (discussed below) the C—Cl stretching mode to be ~688 cm^{-1} for CCl_3 adspecies on a model surface that simulates the Si(1 1 1)7 × 7 surface. Furthermore, this broad feature near 820 cm^{-1} may also have contribution from the Si—C stretching mode, which has been commonly found near 795 cm^{-1}, e.g., as in the case of ethylene/Si(1 1 1) [24].

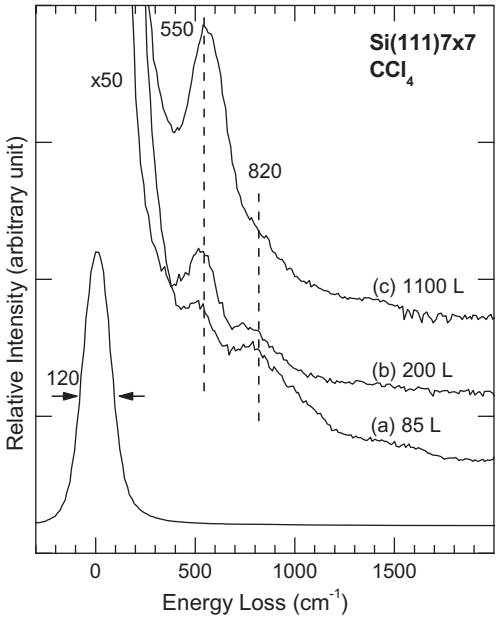

Fig. 1. Vibrational electron energy loss spectra for (a) 85 L, (b) 200 L, and (c) 1100 L of CCl_4 exposed to Si(1 1 1)7 × 7 at room temperature.

Table 1
Comparison of the experimental vibrational electron energy loss energies (in cm^{-1}) for CCl_4 on Si(1 1 1)7 × 7 with free CCl_4 [20], and CCl_4 on Ni(1 1 0) [19], and with those obtained by ab initio calculations based on B3LYP/6-31G(d)) for free CCl_4, and the two adsorbate–substrate configurations (ASCs) on Si(1 1 1)7 × 7

Mode (cm^{-1})	CCl_4/Si(1 1 1)7 × 7 (This work)	CCl_4 vapour Ref. [20]	CCl_4/Ni(1 1 0) Ref. [19]	DFT – B3LYP/6-31G(d) (This work)[c]		
				Isolated CCl_4	ASC A[d]	ASC B
ν(Si—Cl)	550		340[b]		511	580
ν(C—Cl)	N.R[a]	776	720	746	702	683
					677	
ν(Si—C)	820				830	785

[a] Not resolved.
[b] ν(Ni–Cl).
[c] It should be noted that the calculated wavenumbers for the ASCs have not been multiplied by any correction factor as commonly practiced for condensed materials in the literature.
[d] Due to the proximity of one of the Cl atoms of —CCl_3 to the adsorbed Cl atom in ASC A, the ν(C—Cl) vibration mode is found to split into two.

The presence of Si—Cl stretching mode indicates that the CCl_4 molecule undergoes at least partial dechlorination upon adsorption on Si(1 1 1)7 × 7 at RT with the following surface reaction:

$$CCl_4 \rightarrow CCl_x(ad) + (4 - x)Cl(ad)$$

It is however unclear about the extent of the dechlorination, and indeed the presence of different CCl_x ($x < 4$) fragments cannot be

easily inferred from our EELS spectrum. This observation is consistent with the XPS study of CCl_4 on Si(1 0 0) by Junker et al. [5], who exposed the (1 0 0) surface to CCl_4 at 105 K and annealed the sample to 700 K. The Cl 2p feature found at 200.7 eV was attributed to the Cl atoms within the CCl_x ($x \leqslant 4$) fragments. In the present case, adsorption of the resulting CCl_x fragments could occur on Si(1 1 1)7 × 7 through its interaction with the adatom–restatom pair. Further increasing the exposure from 85 L (Fig. 1a) to a higher exposure does not produce additional new EELS features. However, the relative intensity of the Si—Cl feature at 550 cm^{-1} appears to increase while that for C—Cl and/or Si—C feature near 820 cm^{-1} decreases with increasing exposure, suggesting a corresponding increase in the surface Cl moiety with exposure [11]. The very intense peak at 550 cm^{-1} for the 1100 L exposure also appears to overwhelm the nearby features (Fig. 1c). The non-proportional intensity change of these two features with increasing exposure suggests a possible kinetic effect that may favour further dechlorination of the adsorbed CCl_x ($x < 4$) fragments or simultaneous multiple dechlorination upon adsorption of CCl_4 on the 7 × 7 surface. It is of interest to note that CCl_4 is more reactive compared to its smaller tetrahedral homologs, CH_4 [14] and CF_4 [15], on Si(1 1 1)7 × 7. Given that the bond dissociation energies of H—CH_3, F—CF_3, and Cl—CCl_3 are 439, 547, and 297 kJ mol^{-1}, respectively [25], dechlorination of CCl_4 is therefore more energetically favourable than the corresponding processes of dehydrogenation of CH_4 and defluorination of CF_4, but the activation energy is not sufficiently low for the dechlorination to occur at RT. This shows that the activation energy required for Cl dissociation in CCl_4 is lowered due to its interaction with the dangling bonds on Si(1 1 1)7 × 7 at RT. A similar explanation has also been given by Junker et al. [5] for the dissociative adsorption of CCl_4 on Si(1 0 0) at 100 K.

3.2. DFT calculations

The DFT calculations were performed by using the GAUSSIAN 03 package [26], with the assumption that the dissociative adsorption of CCl_4 on Si(1 1 1)7 × 7 leads to CCl_3 and Cl adspecies (i.e. single dechlorination). Given the large number of possible adsorption sites on the 7 × 7 surface, we have chosen only the sites corresponding to the adatom–restatom pair. A $Si_{16}H_{18}$ cluster was used to represent the restatom–adatom sites at the faulted half of the Si(1 1 1)7 × 7 unit cell, after adopting the dimer-adatom-stacking fault model of Takayanagi et al. [9]. The present larger cluster model for the substrate includes the additional 3rd and 4th Si sublayers and should therefore be more reliable than the smaller Si_9H_{12} cluster. The hybrid density functional B3LYP (consisting of Becke's 3-parameter non-local-exchange functional [27] and the correlation functional of Lee–Yang–Parr [28]) along with the standard 6-31G(d), 6-31+G(d), and 6-31++G(d,p) basis sets were employed [26]. The optimal distance between the adatom and restatom was found to be 4.38 Å using the present $Si_{16}H_{18}$ cluster, in good accord with the experiment (~4.5 Å) [9]. Geometry optimization with no constrained degrees of freedom was performed. The reported total energies for the equilibrium adstructures were not corrected for the basis-set superposition error and the zero-point energy.

Assuming single dechlorination upon adsorption, two plausible adsorbate–substrate configurations (ASCs) of the dissociative adspecies on the model surface can be obtained. Fig. 2 shows that CCl_3 and Cl could adsorb on either, respectively, adatom and restatom sites as simulated by the $Si_{16}H_{18}$ cluster (ASC A, Fig. 2a) or vice versa (ASC B, Fig. 2b). The ASC A, with the adsorption energy $\Delta E = -369$ kJ mol^{-1}, is evidently more stable than ASC B, with $\Delta E = -355$ kJ mol^{-1}. As depicted by the more stable ASC A (Fig. 2a), the more electron rich CCl_3 fragment tends to bond with the slightly more electropositive Si adatom site (instead of the slightly more electronegative Si restatom). The corresponding calculated wavenumbers of different vibrational modes for the two ASCs are compared with our EELS data in Table 1. For isolated CCl_4 molecule, the DFT method is found to give good agreement in the wavenumber for ν(C—Cl) (746 cm^{-1}) with that observed experimentally for free CCl_4 (776 cm^{-1}). For the RT dissociative chemisorption of CCl_4, the ν(Si—Cl) wavenumbers for ASC A (511 cm^{-1}) and ASC B (580 cm^{-1}) are similar to the observed feature at 550 cm^{-1} (Fig. 1). A slightly better agreement in the ν(Si—C) wavenumber with the observed peak at 820 cm^{-1} (Fig. 1) is found for ASC A (830 cm^{-1}) than B (785 cm^{-1}). The ν(C—Cl) wavenumbers for the ASC A and ASC B are 677/702 cm^{-1} and 683 cm^{-1} respectively, which do not correspond to any well resolved EELS feature in Fig. 1. This is not surprising because the C—Cl bond is expected to be nearly parallel to the surface, which would lead to rather weak perpendicular dipole-moment component observable in accord with the metal surface selection rule. Given not only the lower total energy and a better agreement in ν(Si—C) wavenumbers, ASC A appears to be the more likely adsorption arrangement. However, these differences between ASC A and ASC B are small and therefore the presence of a minor population of B cannot be ruled out.

3.3. Thermal evolution of adsorption species of CCl_4 on Si(1 1 1)7 × 7

The effect of thermal excitation on the RT adspecies has also been studied for the three CCl_4 exposures of 85 L, 200 L and

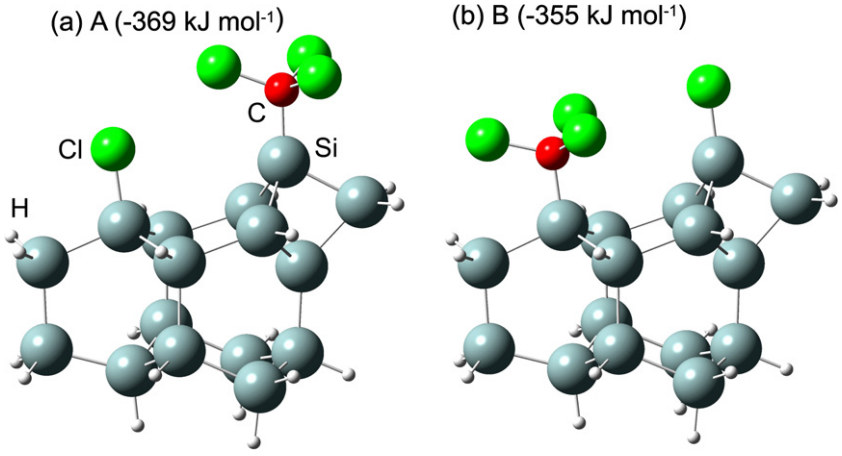

Fig. 2. Optimized geometries and adsorption energies (in parentheses) of two adsorbate–substrate configurations (A, B) for the dissociative adsorption of CCl_4 over a adatom–restatom site on the surface of a $Si_{16}H_{18}$ cluster obtained by a DFT B3LYP/6-31G(d) calculation.

1100 L on Si(1 1 1)7 × 7. Fig. 3A shows that the vibrational EELS spectra for a 85 L RT exposure of CCl_4 on Si(1 1 1)7 × 7 as a function of the sequential flash-annealing temperature up to 983 K. After each flash-anneal, the sample was allowed to cool back to RT before recording the EELS spectrum. Evidently, the ν(Si—Cl) feature at 550 cm^{-1} appears to increase in intensity with increasing annealing temperature, reaching a maximum at 573 K. This intensity increase indicates an increase in the relative concentration of adsorbed chlorine atoms on the 7 × 7 surface, likely due to further Cl dissociation of the adsorbed CCl_x fragments:

$$CCl_x(ad) \rightarrow CCl_{x-1}(ad) + Cl(ad)$$

Further annealing to a higher temperature above 573 K reduces the intensity of the ν(Si—Cl) feature and finally extinguishes it at 983 K, which suggests Cl desorption, likely recombinatively as Cl_2 or alternatively as an etching product $SiCl_y$, from the 7 × 7 surface. The etching of a Si surface by Cl has been previously reported in the thermal desorption study of CCl_4 on Si(1 0 0) by Junker et al. [5], who observed the desorption of the etching product $SiCl_2$ at 880–950 K. The desorption of the latter etching product is thermodynamically feasible, given the bond strengths of Si—Cl (458 kJ mol^{-1}) and Si—Si (75 kJ mol^{-1}) [25].

Furthermore, the feature at 820 cm^{-1} also appears to strengthen with increasing flash-annealing temperature, and a new feature at 920 cm^{-1} is found to emerge at 573 K and remain in the 673 K and 783 K spectra (Fig. 3A). We consider three possible explanations to account for this feature at 920 cm^{-1}. Given that the average wavenumber of a C—C single bond is expected near 950 cm^{-1} [29], the presence of the feature at 920 cm^{-1} may indicate the formation of C—C bond. Brown and Ho [30] reported that moderate exposures of methyl chloride on Si(1 0 0)2 × 1 held above 500 K result in a carbon layer containing C—C single bonds with ν(C—C) at 1050 cm^{-1}. However, the thermal desorption study of CCl_4 on Si(1 0 0) by Junker et al. [5] provided no evidence of C—C bond formation. Alternatively, the 920-cm^{-1} feature may represent the optical surface phonon mode. In particular, the Fuchs–Kliewer mode [31] observed by Dayan [32] for β-SiC(1 0 0) at 116 meV (936 cm^{-1}) was found at a position independent of the SiC surface orientation by Neinhaus et al. [33]. The thickness of the SiC film in these studies [32,33] was greater than 5 μm. In their EELS study of SiC film obtained by heating a C_{60} monolayer on Si(1 1 1)7 × 7 to 900 °C, Sakamoto et al. [34] attributed the EELS peaks at 91 meV (734 cm^{-1}), 102 meV (823 cm^{-1}) and 114 meV (920 cm^{-1}) to the Si—C vibration at the SiC surface, the low-frequency and high-frequency modes of the Fuchs–Kliewer mode, respectively. The Fuchs–Kliewer mode is known [31] to separate into two modes, corresponding to the bulk transverse optical (TO) and longitudinal optical (LO) phonons, with decreasing SiC film thickness. In accord with the assignment made by Sakamoto et al. [34], the features at 820 cm^{-1} and 920 cm^{-1} in Fig. 3A could therefore be attributed to the low-frequency and high-frequency modes of the Fuchs–Kliewer mode, respectively. Sakamoto et al. [34] accounted for the redshift of the high-frequency mode relative to that observed by Dayan [32] to softening of the Si—C bond of the SiC film. The presence of a SiC buffer layer has been proposed to accommodate the lattice mismatch between Si and SiC layers. Finally, the features at 820 cm^{-1} and 920 cm^{-1} could also be due to the formation of SiC alloys as discussed in the ultraviolet photoemission and EELS study of thermal chemistry of acetylene on Si(1 1 1)7 × 7 [35]. In the present work, we have indirect evidence that the feature at 920 cm^{-1} is due to the formation of the SiC film. In particular, we observed an energy gain peak near 920 cm^{-1} in the EELS spectrum for the anneal at 573 K (not shown), which is in good accord with a similar energy gain feature observed by Dayan for β-SiC(1 0 0) [32]. Upon further annealing the sample to 883 K, the feature at 920 cm^{-1} becomes reduced and appears to be merged with the distinct feature that emerges at 820 cm^{-1}, indicating the thermally induced transformation near the surface. The feature at 820 cm^{-1} has been commonly attributed to the Si—C stretching mode [11–13].

The thermal evolutions of the adspecies on Si(1 1 1)7 × 7 for the 200 L (Fig. 3B) and 1100 L exposures of CCl_4 (Fig. 3C) are found to be similar to that for the 85 L exposure (Fig. 3A). Of particular interest is the prominent intensity increase in the ν(Si—Cl) feature at 550 cm^{-1}, which appears to overshadow the higher-lying features at 820 cm^{-1} and 920 cm^{-1} until its complete removal above 883 K. Minor blue shift of the 920-cm^{-1} feature to 960 cm^{-1} at 573–783 K for the 200 L and 1100 L exposures is also observed.

3.4. Thermal evolution of the room-temperature adsorbate as studied by electronic EELS

Fig. 4 shows the electronic EELS spectra of 1000 L exposure of CCl_4 on Si(1 1 1)7 × 7 as deposited at RT and upon sequential flash-annealing to various temperatures. The incident electron energy employed is 100 eV, giving an estimated inelastic mean free path of 5.6 Å [36]. The electronic EELS spectrum of the clean Si(1 1 1)7 × 7 has been studied earlier in both second derivative

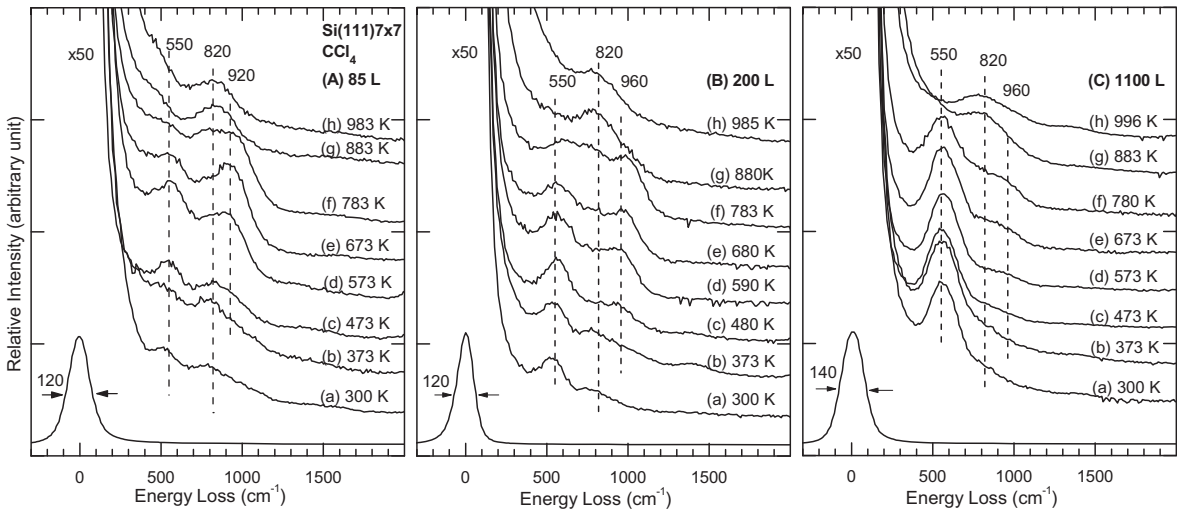

Fig. 3. Vibrational electron energy loss spectra of (A) 85 L, (B) 200 L, and (C) 1100 L of CCl_4 exposed to Si(1 1 1)7 × 7 at (a) room temperature, and upon sequential flash-annealing to (b) 373 K, (c) 473–480 K, (d) 573–590 K, (e) 673–680 K, (f) 780–783 K, (g) 880–883 K, and (h) 983–996 K.

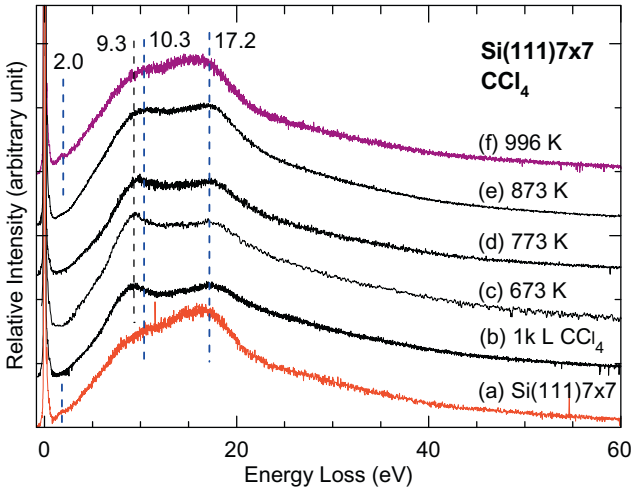

Fig. 4. Electronic electron energy loss spectra of (a) clean Si(1 1 1)7 × 7 and (b) 1000 L of CCl_4 exposed to Si(1 1 1)7 × 7 at room temperature and upon flash-annealing to (c) 673 K, (d) 773 K, (e) 873 K, and (f) 996 K.

mode [10,37–39] and non-derivative mode [40]. The EELS peaks at 2.0 eV, 10.3 eV, and 17.2 eV (Fig. 4a) have been assigned to the transitions from the occupied surface states, surface plasmon, and bulk plasmon, respectively, of the Si substrate [37]. Upon exposure of 1000 L of CCl_4 to the 7 × 7 surface, a new EELS feature at 9.3 eV is clearly evident (Fig. 4b). This electronic feature at 9.3 eV remains prominent even after annealing the sample to 673 K, and it becomes weaken and eventually completely diminished upon further annealing to 996 K. Given that the ν(Si—Cl) feature at 550 cm^{-1} (Fig. 3C) is found to persist even after annealing to 780 K and its thermal evolution appears to correlate well with the feature at 9.3 eV, the latter feature could be related to the formation of Si—Cl bond. In the electronic EELS study of adsorption of HCl on Si(1 1 1) reported by Miyamura et al. [10], ~5 L HCl on Si(1 1 1) was annealed to ~800 K. Three transitions at 6.0 eV, 7.0 eV, and 9.0 eV were observed (in second derivative mode) and have been attributed to the formation of stable Si—Cl bond. The initial states of the transitions at 6.0 eV and 7.0 eV and at 9.0 eV were assigned to the Cl π-bonding states and σ-like bonding states, respectively, while the final states for all three transitions were 1.0 eV above the bottom of the conduction band. The assignment of the electronic feature at 9.3 eV in the present work (Fig. 4) is therefore consistent with that for the transition at 9.0 eV reported by Miyamura et al. [10]. In the electronic EELS study of Cl_2 on Si(1 1 1)7 × 7 by Aoto et al. [38,39], the EELS feature observed at 8.8 eV (in second derivative mode) was attributed to the single-electron transition from the Cl(p_z) bonding state [that makes a σ-like bonding state with the Si(p_z) state] to the Cl(p_z) antibonding state produced by the Si—Cl bond. We therefore propose that the origin of the EELS feature at 9.3 eV in Fig. 4 as being similar to that of the 8.8 eV peak reported by Aoto et al. [38,39]. Finally, in an earlier study of the electronic structure of Si(1 1 1)–Cl by angle resolved EELS [41], Best reported an EELS peak at 8.7 eV and further attributed it to a superposition of two electron transitions: One from the Cl(p_z) state that makes a σ-like bonding state with the Si(p_z) to the Cl(p_z) antibonding state, and another from the Cl(p_x,p_y) state that makes a π-like bonding state to the Cl(p_z) antibonding state. Finally, upon annealing the sample to 996 K, the resulting EELS spectrum (Fig. 4f) becomes almost identical to that of the clean Si(1 1 1)7 × 7 (Fig. 4a), with the reappearance of the surface state at 2.0 eV. Apparently, the electronic EELS spectrum does not appear to be sufficiently sensitive to reveal any carbon-related EELS feature [40] in the annealed sample.

4. Conclusions

Like Si(1 0 0) [4–7], carbon tetrachloride is found in the present work to undergo dissociative adsorption on Si(1 1 1)7 × 7 at room temperature with the formation of the Si—Cl bond. The extent of dechlorination of CCl_4 on Si(1 1 1)7 × 7 at RT is likely to increase with increasing exposure. Furthermore, CCl_4 is found to be more reactive than CH_3Cl [16] on Si(1 1 1)7 × 7 at RT. Our DFT calculations further show that the adsorption arrangement corresponding to the Cl and CCl_3, respectively, on the restatom and adatom sites appears to give the lowest adsorption energy. The corresponding calculated vibrational wavenumbers are found to be comparable to the experimental vibrational EELS data. Annealing the sample to 573–783 K results in a new EELS feature at 920 cm^{-1}, which can be attributed to the formation of SiC film or alloy, suggesting that CCl_4 could be used as a viable carbon source for SiC film growth. The dissociated Cl atoms on the Si surface can be completely removed by annealing to 883 K. The companion electronic EELS study reveals a Cl-related EELS peak at 9.3 eV that could be assigned to the electron transition between the Cl(p_z) bonding and antibonding states of the Si—Cl bond. To our knowledge, the present work represents the first such study that collaborates the electronic transition related to Si—Cl σ bond with the vibrational data of the Si—Cl stretching mode. Further comparative studies of the interactions of the chlorinated methanes (CH_2Cl_2, $CHCl_3$) and of other tetrahalocarbons (CBr_4 and Cl_4) on Si(1 1 1)7 × 7 could provide further insights into the intricate halogen surface chemistry on silicon.

Acknowledgement

This work was supported by the Natural Sciences and Engineering Research Council of Canada.

References

[1] T. Nyberg, P. Heszler, J.O. Carlsson, Diamond Relat. Mater. 6 (1997) 85.
[2] T.P. Chow, P.A. Maciel, G.M. Fanelli, J. Electrochem. Soc. 134 (1987) 1281.
[3] S. Hascik, P. Elias, J. Soltys, J. Martaus, Czech. J. Phys. 56 (2006) B1169.
[4] C.L. French, R.B. Jackman, R.J. Price, J.S. Foord, J. Phys.: Condens. Matter 1 (1989) SB181.
[5] K.H. Junker, G. Hess, J.G. Ekerdt, J.M. White, J. Vac. Sci. Technol. A 16 (1998) 2995.
[6] K.H. Junker, J.M. White, J. Vac. Sci. Technol. A 16 (1998) 3328.
[7] A.T.S. Wee, C.H.A. Huan, K.L. Tan, R.S.K. Tan, J. Mater. Sci. 29 (1994) 4037.
[8] V. Liberman, G. Haase, R.M. Osgood Jr., Surf. Sci. 268 (1992) 307.
[9] K. Takayanagi, T. Tanishiro, S. Takahashi, M. Takahashi, J. Vac. Sci. Technol. A 3 (1985) 1502.
[10] M. Miyamura, Y. Sakisaka, M. Nishijima, M. Onchi, Surf. Sci. 72 (1978) 243.
[11] Z. He, K.T. Leung, Surf. Sci. 583 (2005) 179.
[12] Z. He, Q. Li, K.T. Leung, J. Phys. Chem. B 109 (2005) 14908.
[13] Z. He, Q. Li, K.T. Leung, Surf. Sci. 600 (2006) 514.
[14] J.K. Simons, S.P. Frigo, J.W. Taylor, R.A. Rosenberg, Surf. Sci. 346 (1996) 21.
[15] Z. He, K.T. Leung, Appl. Surf. Sci. 174 (2001) 225.
[16] R. Kuester, K. Christmann, Ber. Bunsen-Ges. Phys. Chem. 101 (1997) 1799.
[17] L.J. Whitman, S.A. Joyce, J.A. Yarmoff, F.R. McFeely, L.J. Terminello, Surf. Sci. 232 (1990) 297.
[18] D. Hu, Ph.D. Thesis, University of Waterloo, Waterloo, Ontario, Canada, 1993.
[19] M.A. Chesters, D. Lennon, Surf. Sci. 426 (1999) 92.
[20] T. Shimanouchi, Tables of Molecular Vibrational Frequencies Consolidated, Vol. 1, National Bureau of Standards, Washington, DC, 1972. pp. 1–160.
[21] Q. Gao, C.C. Cheng, P.J. Chen, W.J. Choyke, J.T. Yates Jr., J. Chem. Phys. 98 (1993) 8308.
[22] K. Nishiyama, Y. Tanaka, H. Harada, T. Yamada, D. Niwa, T. Inoue, T. Homma, T. Osaka, I. Taniguchi, Surf. Sci. 600 (2006) 1965.
[23] O.B. Koper, E.A. Wovchko, J.A. Glass, J.T. Yates Jr., K.J. Klabunde, Langmuir 11 (1995) 2054.
[24] J. Yoshinobu, H. Tsuda, M. Onchi, M. Nishijima, Solid State Commun. 60 (1986) 801.
[25] Y.-R. Luo, Comprehensive Handbook of Chemical Bond Energies, CRC Press, Taylor & Francis Group, 2007.
[26] M.J. Frisch, G.W. Trucks, H.B. Schlegel, G.E. Scuseria, M.A. Robb, J.R. Cheeseman, J.A. Montgomery Jr., T. Vreven, K.N. Kudin, J.C. Burant, J.M. Millam, S.S. Iyengar, J. Tomasi, V. Barone, B. Mennucci, M. Cossi, G. Scalmani, N. Rega, G.A. Petersson, H. Nakatsuji, M. Hada, M. Ehara, K. Toyota, R. Fukuda, J. Hasegawa,

M. Ishida, T. Nakajima, Y. Honda, O. Kitao, H. Nakai, M. Klene, X. Li, J.E. Knox, H.P. Hratchian, J.B. Cross, C. Adamo, J. Jaramillo, R. Gomperts, R.E. Stratmann, O. Yazyev, A.J. Austin, R. Cammi, C. Pomelli, J.W. Ochterski, P.Y. Ayala, K. Morokuma, G.A. Voth, P. Salvador, J.J. Dannenberg, V.G. Zakrzewski, S. Dapprich, A.D. Daniels, M.C. Strain, O. Farkas, D.K. Malick, A.D. Rabuck, K. Raghavachari, J.B. Foresman, J.V. Ortiz, Q. Cui, A.G. Baboul, S. Clifford, J. Cioslowski, B.B. Stefanov, G. Liu, A. Liashenko, P. Piskorz, I. Komaromi, R.L. Martin, D.J. Fox, T. Keith, M.A. Al-Laham, C.Y. Gonzalez, J.A. Pople, Gaussian 03 Revision A.1, Gaussian, Inc., Pittsburgh, PA, 2003.
[27] A.D. Becke, J. Chem. Phys. 98 (1993) 5648.
[28] C. Lee, W. Yang, R.G. Parr, Phys. Rev. B 37 (1989) 785.
[29] H. Ibach, D.L. Mills, Electron Energy Loss Spectroscopy and Surface Vibrations, Academic Press, New York, 1982. p. 197.
[30] K.A. Brown, W. Ho, Surf. Sci. 338 (1995) 111.
[31] R. Fuchs, K.L. Kliewer, Phys. Rev. A 140 (1965) 2076.
[32] M. Dayan, Surf. Sci. 149 (1985) L33.
[33] H. Neinhaus, T.U. Kampen, W. Monch, Surf. Sci. 324 (1995) L328.
[34] K. Sakamoto, T. Suzuki, T. Wakita, S. Suto, C.W. Hu, T. Ochiai, A. Kasuya, Appl. Surf. Sci. 121/122 (1997) 200.
[35] V. De Renzi, R. Biagi, U. del Pennino, Phys. Rev. B 64 (2001) 155305-1.
[36] W.S.M. Werner, Surf. Interf. Anal. 31 (2001) 141.
[37] H. Ibach, J.E. Rowe, Phys. Rev. B 9 (1974) 1951.
[38] N. Aoto, E. Ikawa, Y. Kurogi, Surf. Sci. 199 (1988) 408.
[39] N. Aoto, E. Ikawa, T. Kikkawa, Y. Kurogi, Surf. Sci. 250 (1991) 235.
[40] H. Yu, K.T. Leung, Surf. Sci. 432 (1999) 245.
[41] P.E. Best, Phys. Rev. B 19 (1979) 1054.